# Coplanar Bithiazole-Centered Heterocyclic Aromatic Fluorescent Compounds Having Different Donor/Acceptor Terminal Groups

Tao Tao, Yu-Xin Peng, Wei Huang,* and Xiao-Zeng You

State Key Laboratory of Coordination Chemistry, Nanjing National Laboratory of Microstructures, School of Chemistry and Chemical Engineering, Nanjing University, Nanjing 210093, P. R. China

S Supporting Information

ABSTRACT: A family of stable and soluble bithiazole-centered heterocyclic aromatic fluorescent compounds is described herein. All these multiple N-donor containing compounds have effective π-conjugated systems and different imidazole, pyridine, thiophene, triphenylamino, benzoic acid, and ethyl benzoate tails showing distinguishable D−A−A−D and A−A−A−A structures. X-ray single-crystal structures of seven compounds indicate that all of the bithiazole cores have the same *trans* coplanar configuration but exhibit different dihedral angles with their adjacent aromatic heterocycles $(4.5(6)−69.7(3)°)$. Optical and electrochemical results demonstrate that the TPA-terminated bithiazole compound **2TPA2TZ** has yellow fluorescence and reversible redox activity as well as extraordinarily high thermal stability. Theoretical and experimental studies have been made to reveal the differences from related compounds with adjustable electronic properties. The internal reorganization energy (λ) studies have been carried out to indicate the differences between the bithiazole-based derivatives and the corresponding bithiophene-based counterparts.
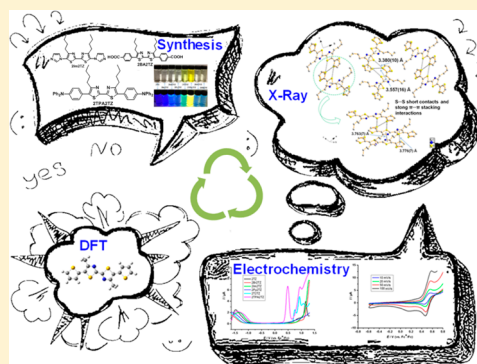
INTRODUCTION

In recent years, linear π-conjugated semiconducting compounds have been extensively studied in the field of molecular-based materials[1] such as organic and polymeric light emitting diodes,[2] field effect transistors,[3] and photovoltaic cells.[4] Compared with the corresponding polydisperse polymers, the monodisperse oligomers are excellent model compounds and have many advantages including their well-defined chemical structures, better solubility, easier purification, fewer defects, greater synthetic reproducibility, and the possibility of introducing versatile functionalities.[5] However, all these present both opportunities and challenges to rational design and synthesis of extended heterocyclic aromatic systems for constructing high-performance electronic materials.

Thiophene-/thiazole-containing conjugated oligomers represent an intriguing and promising class of materials because they are believed to be ideal functional elements and building blocks in the studies of molecular electronics.[6] More importantly, the enormous and attractive potential of structural variations makes possible the fine-tuning of optoelectronic properties in a wide range.[7] However, the device applicability of such materials can be influenced by various factors, including narrow energy gap, appropriate highest occupied molecular orbital (HOMO) and lowest unoccupied molecular orbital (LUMO) energy levels, high thermal durability, ease for the mobility of hole and electron, and the geometrical packing in the solid state.[8] Thus, X-ray single-crystal diffraction, which is believed to be a bridge between theory and experiment, has been proved to be one of

the most powerful tools to characterize the molecular geometry and packing for organic small molecules.[9]

In our previous work, a series of 1,10-phenanthroline-based and oligothiophene-based heterocyclic aromatic compounds with terminal thienyl, imidazolyl, and pyridyl groups has been described.[10] Furthermore, temperature-dependent semiconducting and photoresponsive properties of self-assembled nanocomposite films and nanodevices fabricated from these compounds and their metal complexes have been explored.[11] In view of relatively fewer investigations on the thiazole-based semiconducting heterocyclic aromatic derivatives in comparison with the thiophene-based ones, we have extended our work herein on the bithiazole-centered semiconducting and fluorescent compounds with the same coplanar core and two chelating nitrogen atoms as the coordination sites, bearing various electron-donating and electron-withdrawing tails, namely bromo, imidazolyl, pyridyl, thienyl, triphenylamino, benzoic acid, and ethyl benzoate groups (Scheme 1). Two *n*-butyl chains are introduced herein on the β-position of each bithiazole unit in order to (a) increase the solubility in conventional organic solvents but minimize the effect on the increase of molecular planarity, (b) facilitate the related C−C bond and C−N bond cross-coupling reactions and improve the final yields, (c) enhance the weak donor property of the thiazole ring.

Scheme 1. Synthetic Route of Bithiazole-Based Heterocyclic Aromatic Fluorescent Compounds
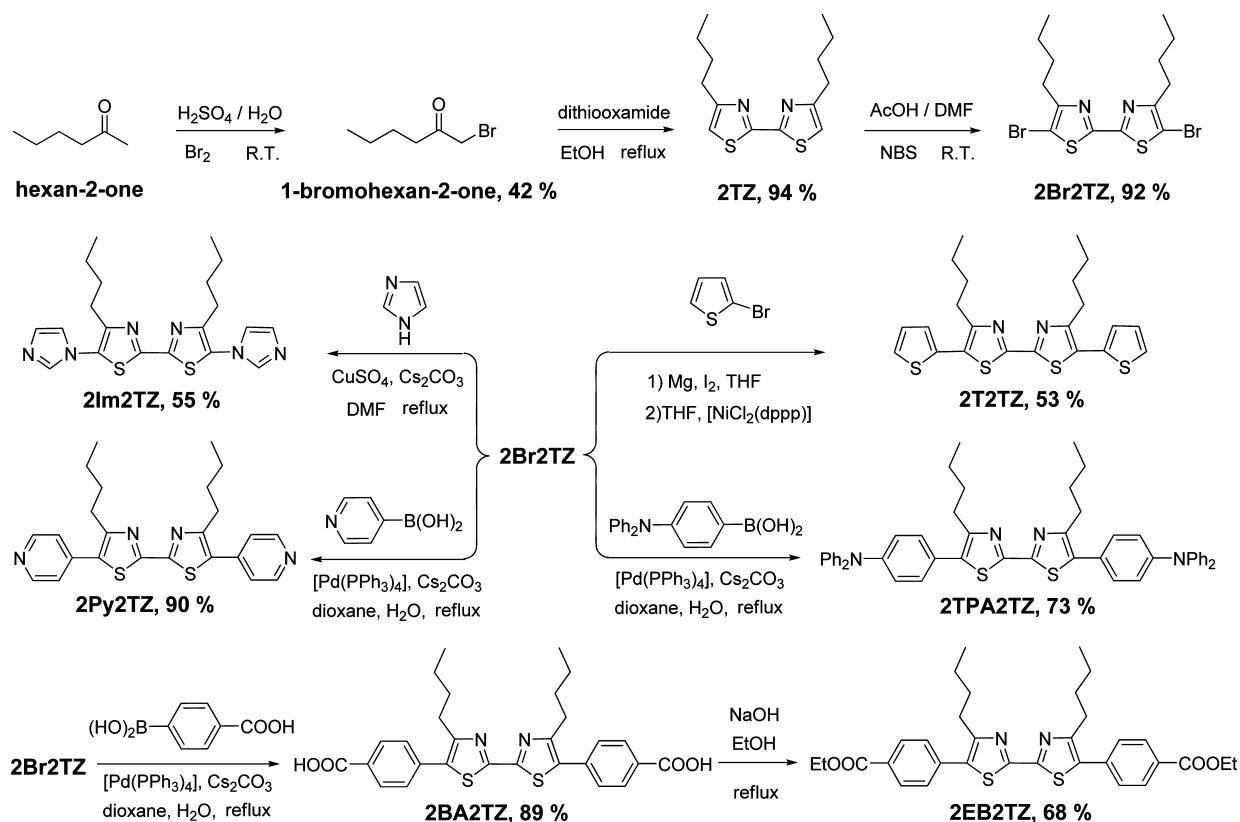
The aim of incorporating various donor and acceptor substituents into one molecule is to finely tune their electronic structures and compare their spectroscopic, electrochemical, and thermal properties. The acquirement of these linear heterocyclic aromatic compounds especially the single-crystal structures prompts us to further explore the possible rules between their structures and properties, for example, the relationship between the number of aromatic heterocycles and the electronic and fluorescence spectra, energy gap alterations, the limitation of solubility of compounds which is also influenced by the substituent effects. In addition, theoretical and experimental studies have been carried out to reveal the differences between the bithiazole-based derivatives and the corresponding bithiophene-based counterparts.

■ RESULTS AND DISCUSSION

Syntheses and Spectral Characterizations. Our synthetic strategy was based on the routes shown in Scheme 1, in which the starting material 5,5′-dibromo-4,4′-dibutyl-2,2′-bithiazole (**2Br2TZ**) was prepared according to the previously reported approaches.[12] All the target compounds were prepared by carbon–carbon (C–C) bond or carbon–nitrogen (C–N) bond cross-coupling reactions. The use of different cross-coupling methods, such as Kumada–Corriu, Suzuki–Miyaura, and Ullmann reactions, have been carried out to optimize the experimental conditions in order to prepare the linear π-conjugated compounds with high yields. As shown in Figures SI1–9 (Supporting Information), all the heterocyclic aromatic compounds have been characterized by ^{1}H, ^{13}C NMR and EI-TOF-MS spectra, and the results clearly demonstrate the formation of the expected compounds.

In comparison with bithiazole bearing no substituent, our results demonstrate that the introduction of two *n*-butyl chains on the *β*-position of each thiazole ring can effectively increase the solubility in conventional organic solvents but minimize the effect on the increase of molecular planarity, facilitate the related C–C bond and C–N bond cross-coupling reactions, improve the final yields, and enhance the weak donor property of the thiazole ring. As a result, the benzoic acid extended bithiazole compound **2BA2TZ** can be successfully prepared by the Suzuki–Miyaura reaction in a high yield of 89%. However, the solubility of this compound is still not good enough in chloroform. To solve this problem and keep its electronic structure, compound **2EB2TZ** was synthesized by the conventional ethyl esterification in a yield of 68%. It is worth mentioning that **2EB2TZ** has been further confirmed by the ^{1}H–^{1}H and ^{1}H–^{13}C correlation spectroscopy (COSY) NMR shown in Figures SI9c and SI9d (Supporting Information). As anticipated, triphenylamino- and pyridyl-terminated compounds **2TPA2TZ** and **2Py2TZ** were synthesized with satisfactory yields in the presence of $[Pd(PPh_3)_4]$ catalyst by using a strong cross-coupling reagent, i.e. 4-(diphenylamino)-phenylboronic acid and 4-pyridinylboronic acid. As shown in Scheme 1, thiophene-terminated bithiazole compound **2T2TZ** was also first prepared by the classical C–C bond cross-coupling reaction by the treatment of Grignard reagents obtained from corresponding bithiazole-based bromides and magnesium turnings in the presence of $[NiCl_2(dppp)]$ catalyst in dry THF in a yield of 53%.

As illustrated in Figure 1, all new compounds show characteristic absorptions at 332–408 nm in their electronic spectra corresponding to the π–π* transitions between adjacent aromatic heterocycles. The strong absorption peak at
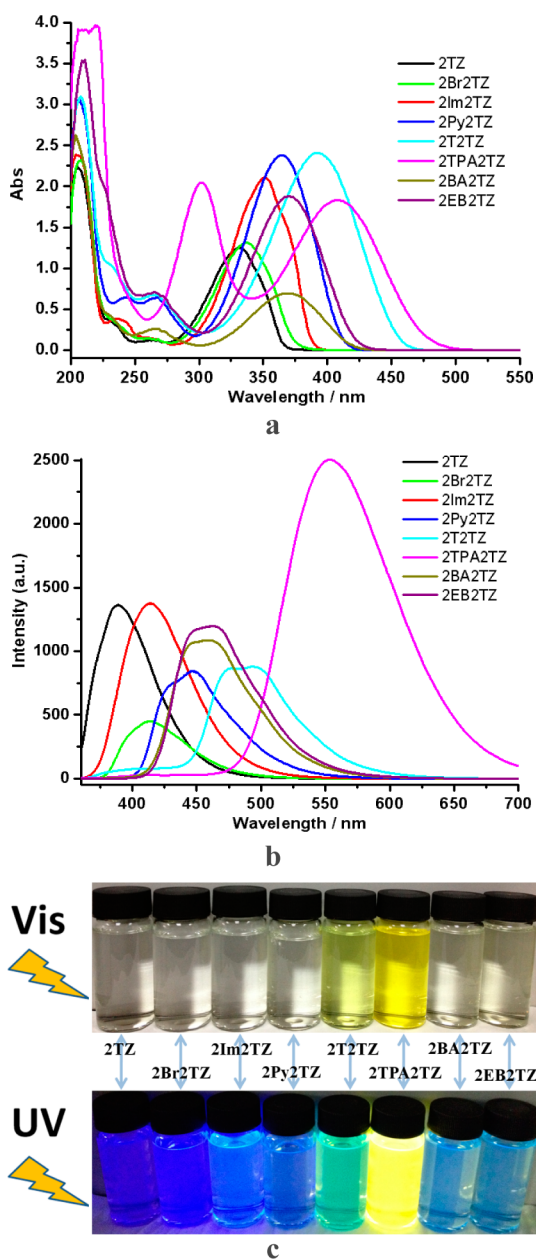
Figure 1. UV−vis absorption spectra (a), fluorescence emission excited at 350 nm (b), and their visual photographs (c) for the heterocyclic aromatic compounds in their methanol solutions at room temperature with the same concentration of 5.0×10^{-5} mol·L^{-1}.

high-energy band (302 nm) for **2TPA2TZ** is assigned as the interring electronic transitions among the three phenyl rings of TPA. Moreover, this family of linear heterocyclic aromatic compounds is fluorescent active. In particular, compound **2TPA2TZ** shows an extraordinarily strong fluorescence peak at 554 nm with the luminescence quantum yield (Φ) of 22% by using anthracene as a standard (Φ_{std} = 27%, see the Supporting Information). At the same time, it exhibits a strong UV−vis absorption peak at 408 nm (ε = 36700 L·mol^{-1}·cm^{-1}). In comparison with compound **2TZ**, similar bathochromic shifts have been found in the fluorescence emission spectra of compounds **2Im2TZ**, **2Py2TZ**, and **2T2TZ** when the number of aromatic heterocycles (namely delocalized π-systems) is increased. In addition, compounds **2BA2TZ** and **2EB2TZ** show similar λ_{max} in the UV−vis absorption and fluorescence

emission spectra. However, the molar extinction coefficient of **2BA2TZ** (ε = 13900 L·mol^{-1}·cm^{-1}) is less than that of **2EB2TZ** (ε = 37600 L·mol^{-1}·cm^{-1}) as depicted in Figure 1a and Table 1. Compared with the oligothiophene-based aromatic heterocyclic compounds[10d] showing characteristic fluorescence emissions, red-shifts are observed for these bithiazole-based counterparts to different extents especially for the pyridyl-, thienyl-, and triphenylamino-terminated bithiazole compounds.

Single-Crystal and Molecular Packing Structures. In this work, we tried to obtain as many single-crystal structures of our compounds as possible in order to fully characterize their molecular geometry and further illuminate and compare their packing modes and supramolecular interactions. As a result, single-crystal structures of seven compounds, i.e., **2TZ**, **2Br2TZ**, **2Im2TZ**, **2Py2TZ**, **2T2TZ**, **2BA2TZ**, and **2EB2TZ** (Tables 2 and SI1, Supporting Inforamtion), have been obtained. It is interesting to mention that the central two thiazole rings of all the compounds are found to adopt the same coplanar and *trans* configuration. However, the coplanar bithiazole cores display different dihedral angles with their adjacent aromatic heterocycles to reduce the steric hindrance as depicted in Figure 2.

On the one hand, they all have many *N*-donors in their molecular structures such as bithiazole, imidazole and pyridine units. On the other hand, compounds **2Im2TZ** and **2Py2TZ** have the alternate A−A−A−A heterocyclic aromatic system, while compound **2T2TZ** shows a distinguishable D−A−A−D structure. On the basis of the two aforementioned aspects, it is possible for us to finely tune their optoelectronic properties by introducing a variety of metal ions by means of the formation of coordinative bonds.

The molecular lengths of linear compounds **2Im2TZ**, **2Py2TZ**, **2T2TZ**, **2BA2TZ**, and **2EB2TZ** are longer than 1.33 nm. It is noted that these molecules show good planarity except compound **2Im2TZ**. The stereochemistry and conformation of **2Im2TZ** may be interesting in forming the hydrogen-bonding contacts and coordinative bonds because of the free rotation of the C−N single bonds between the two side imidazole rings and the central bithiazole plane.[10c] The crystal structure of **2Im2TZ** herein displays the *trans/trans/trans* conformation and the two side imidazole rings are not coplanar to the central bithiazole unit with the same dihedral angle as large as 69.7(3)°. It is believed that the increase of intramolecular planarity, which could reduce the reorganization energy and enhance the electronic coupling between adjacent molecules, would be much more efficient for the transportation of charge carriers.[13] For this reason, it is predicted that **2Im2TZ** has larger reorganization energy than others due to its large dihedral angles between the thiazole and the imidazole rings in the solid state, and this turns out to be true from the following reorganization energy calculations for this family of compounds.

The crystal-packing view of this family of linear heterocyclic aromatic compounds is also shown in Figure 3 and Figure SI10 (Supporting Information), where the intermolecular hydrogen bonding and π−π stacking interactions are found. It is worth mentioning that the packing structure of **2T2TZ** has the multiple S···S short contacts (3.380(10) and 3.557(16) Å) and strong π−π stacking interactions between neighboring thiazole/thiazole and thiazole/thiophene rings with the centroid-to-centroid separations of 3.763(3) and 3.776(7) Å, respectively.

Table 1. UV-Vis Absorption and Fluorescence Emission Data, Optical, Electrochemistry, Calculated HOMO−LUMO Energy Gaps (Eg), and Internal Reorganization Energy (λ) for Related Heterocyclic Aromatic Compounds

compd	UV−vis λ_{max} [nm (eV)]	ε (L·mol^{-1}·cm^{-1})	$Eg^{opt\,a}$ (eV)	$Eg^{calcd\,b}$ (eV)	fluorescence λ_{max} (nm)	$Td_{10}{}^{c}$ (°C)	$E_{ox}{}^{onset\,d}$ (V)	$E_{HOMO}{}^{e}$ (eV)	$E_{LUMO}{}^{f}$ (eV)	$\lambda_{2TZ}{}^{g}$ (eV)	$\lambda_{2T}{}^{h}$ (eV)
2TZ	332 (3.73)	25000	3.42	4.16	389	171	0.68	−5.78	−2.36	0.39	0.36
2Br2TZ	338 (3.67)	26300	3.32	3.88	413	205	1.06	−6.16	−2.84	0.39	0.35
2Im2TZ	352 (3.52)	42200	3.22	3.84	414	238	0.94	−6.04	−2.82	0.78	0.73
2Py2TZ	365 (3.40)	47700	3.04	3.59	447	299	0.61	−5.71	−2.67	0.34	0.27
2T2TZ	393 (3.16)	48300	2.74	3.05	494	258	0.62	−5.72	−2.98	0.31	0.29
2TPA2TZ	408 (3.04)	36700	2.60	3.07	554	437	0.35	−5.45	−2.85	0.40	0.34
2BA2TZ	370 (3.35)	13900	2.97	3.46	458	268	0.95	−6.05	−3.08	0.36	0.30
2EB2TZ	370 (3.35)	37600	2.96	3.46	463	296	0.82	−5.92	−2.96	0.37	0.30

[a]Optical energy gap determined from the UV−vis absorptions in solution. [b]The geometries are calculated by the B3LYP method and 6-31G* basis set. [c]10% weight loss temperature. [d]Oxidation onset potentials determined from DPV vs Fc/Fc^{+}. [e]Calculated from $E_{HOMO} = -(E_{ox}{}^{onset} + 5.10)$. [f]Calculated from $E_{LUMO} = E_{HOMO} + Eg^{opt}$. [g]Calculated the internal reorganization energy for bithiazole-based model compounds. [h]Calculated the internal reorganization energy for bithiophene-based compounds.

Table 2. Crystal Data and Structure Refinements for Seven Compounds: 2TZ, 2Br2TZ, 2Im2TZ, 2Py2TZ, 2T2TZ, 2BA2TZ, and 2EB2TZ

compd	2TZ	2Br2TZ	2Im2TZ	2Py2TZ	2T2TZ	2BA2TZ·(DMF)$_2$	2EB2TZ
formula	$C_{14}H_{20}N_2S_2$	$C_{14}H_{18}Br_2N_2S_2$	$C_{20}H_{24}N_6S_2$	$C_{24}H_{26}N_4S_2$	$C_{22}H_{24}N_2S_4$	$C_{28}H_{28}N_2O_4S_2\cdot(C_3H_7NO)_2$	$C_{32}H_{36}N_2O_4S_2$
formula wt	280.46	438.24	412.59	434.63	444.71	666.86	576.77
T (K)	291(2)	291(2)	291(2)	291(2)	291(2)	291(2)	291(2)
wavelength/Å	0.71073	0.71073	0.71073	0.71073	0.71073	0.71073	0.71073
cryst size (mm)	0.12 × 0.12 × 0.14	0.10 × 0.12 × 0.12	0.10 × 0.12 × 0.12	0.10 × 0.11 × 0.12	0.10 × 0.11 × 0.11	0.10 × 0.13 × 0.15	0.10 × 0.11 × 0.11
cryst syst	monoclinic	triclinic	monoclinic	triclinic	monoclinic	triclinic	triclinic
space group	$P2_1/c$	$P\bar{1}$	$P2_1/c$	$P\bar{1}$	$P2_1/c$	$P\bar{1}$	$P\bar{1}$
a (Å)	8.103(2)	5.142(1)	13.393(2)	5.4824(15)	5.175(13)	5.4606(19)	8.436(6)
b (Å)	9.953(3)	8.5329(17)	8.3690(14)	9.311(3)	25.53(6)	12.111(4)	9.551(7)
c (Å)	10.356(4)	9.860(2)	10.1189(16)	11.760(3)	9.45(2)	14.081(5)	10.274(7)
α (deg)	90	84.688(3)	90	82.339(4)	90	100.073(5)	102.203(9)
β (deg)	116.195(4)	83.755(2)	107.022(2)	77.410(3)	117.87(4)	96.591(7)	105.772(9)
γ (deg)	90	85.838(3)	90	73.259(4)	90	101.281(6)	100.009(9)
V (Å^3)	749.4(4)	427.35(15)	1084.5(3)	559.4(3)	1104(4)	888.4(5)	754.7(9)
Z/D_{calcd} (g/cm^3)	2/1.243	1/1.703	2/1.263	1/1.290	2/1.338	1/1.247	1/1.269
F(000)	300	218	436	230	468	354	306
μ (mm^{-1})	0.341	4.978	0.263	0.256	0.441	0.198	0.215
max/min transmission	0.9603/0.9538	0.6359/0.5865	0.9742/0.9691	0.9748/0.9699	0.9572/0.9531	0.9805/0.9710	0.9788/0.9767
h_{min}/h_{max}	−8/9	−6/6	−15/14	−6/6	−6/6	−6/4	−10/7
k_{min}/k_{max}	−11/10	−10/7	−7/9	−11/10	−30/19	−13/14	−11/11
l_{min}/l_{max}	−12/10	−11/11	−12/12	−12/13	−11/11	−16/16	−10/12
data/param	1317/83	1467/93	1896/128	1931/137	1932/184	2850/222	2623/184
final R indices [$I > 2\sigma(I)$]^a	R1 = 0.0486 wR2 = 0.1337	R1 = 0.0535 wR2 = 0.1319	R1 = 0.0385 wR2 = 0.1104	R1 = 0.0454 wR2 = 0.1174	R1 = 0.0918 wR2 = 0.2119	R1 = 0.0908 wR2 = 0.2409	R1 = 0.0354 wR2 = 0.0763
R indices (all data)^a	R1 = 0.0519 wR2 = 0.1386	R1 = 0.0574 wR2 = 0.1344	R1 = 0.0486 wR2 = 0.1174	R1 = 0.0596 wR2 = 0.1270	R1 = 0.1891 wR2 = 0.2475	R1 = 0.1748 wR2 = 0.2773	R1 = 0.0528 wR2 = 0.0823
S	1.06	1.05	1.10	0.97	0.95	1.05	0.92
max/min Δρ (e·Å^{-3})	0.51/−0.38	1.10/−1.17	0.21/−0.22	0.22/−0.43	0.28/−0.30	0.31/−0.37	0.15/−0.16

$^aR1 = \Sigma||F_o| - |F_c||/\Sigma|F_o|$, $wR2 = [\Sigma[w(F_o{}^2 - F_c{}^2)^2]/\Sigma w(F_o{}^2)^2]^{1/2}$.

Thermal Stability. Thermal durability of π-conjugated small molecules has significant impact on the device performance, which is one of the most essential parameters for the fine-tuned optoelectronic applicability.[14] In this work, eight bithiazole-based aromatic heterocyclic compounds have been checked by the TGA measurements, and a parameter of Td_{10} (10% weight-loss temperature) is used to describe the thermal stability of these compounds. As shown in Figure 4, the TGA curves of **2Br2TZ, 2Im2TZ, 2Py2TZ, 2T2TZ, 2TPA2TZ, 2BA2TZ,** and **2EB2TZ** indicate that they can remain unchangeable when the temperature is below 200 °C and the Td_{10} values for them are found to range from 205 to 437 °C. Furthermore, the bithiazole derivatives **2Py2TZ, 2EB2TZ,** and **2TPA2TZ** show higher performance in the thermal stability compared with other bithiazole-based compounds. In particular, the Td_{10} value for the TPA-extended bithiazole compound **2TPA2TZ** is 437 °C, indicative of excellent thermal stability.

Electrochemical Properties. It is generally believed that the HOMO of the D−A oligomer is determined by the HOMO of the donor unit, while the LUMO of D−A oligomer is
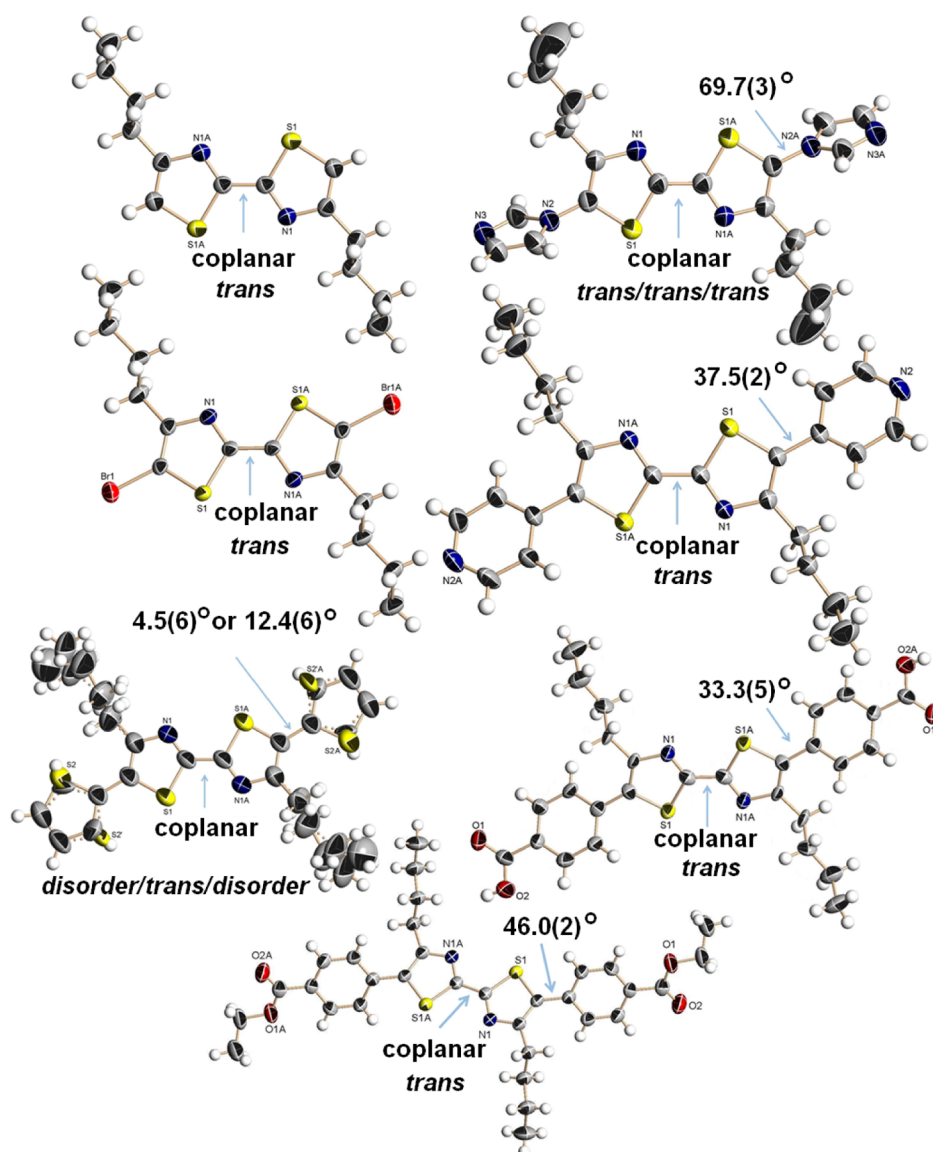
Figure 2. ORTEP diagrams (30% thermal probability ellipsoids) of the molecular structures of **2TZ**, **2Br2TZ**, **2Im2TZ**, **2Py2TZ**, **2T2TZ**, **2BA2TZ**, and **2EB2TZ** showing the dihedral angles and relative configurations between adjacent aromatic heterocycles.

controlled by the LUMO of acceptor unit.[15] Therefore, the electrochemical behavior of bithiazole-based heterocyclic aromatic compounds was examined by the cyclic voltammetry (CV) and the differential pulse voltammetry (DPV) measurements in their 1.0×10^{-3} mol·L^{-1} CH$_2$Cl$_2$ solutions containing 0.1 mol·L^{-1} TBAClO$_4$ as the supporting electrolyte at different scan rates (10, 20, 50, and 100 mV·s^{-1}). All potentials reported herein were calibrated with the ferrocene/ferrocenium couple (Fc/Fc$^+$) as internal standard. Oxidation onset potentials (E_{ox}^{onset}) as well as HOMO/LUMO energy levels were determined by the DPV and absorption data, which are summarized in Table 1. The onset oxidation was measured relative to the Fc/Fc$^+$ couple where an energy level of -5.10 eV versus vacuum was assumed.[16]

As depicted in Figures 5a, compound **2TPA2TZ** shows reversible and well-defined redox response in the CV measurements. However, the other bithiazole derivatives do not present good enough electrochemical activity in the CV experiments, which are consistent with previously reported[17] bithiazole oligomers. Consequently, the DPV method is used to

further explore the electrochemical properties for related compounds in this case. As can be seen in Figure 5b, one or two oxidation waves have been observed for all compounds, and the oxidation potentials and the measured currents are found to be dependent on their molecular structures. The first oxidation wave can be attributed to the formation of cation-radical species and the second one is ascribed to the successive oxidation of cation-radical to its corresponding dication, which have been observed previously in other thiophene and thiazole compounds.[17,18] In particular, compound **2T2TZ** displays three oxidation waves in the range 0.7–1.2 V, indicative of the existence of three stable cation-radical species, which are suggested to be the first and the second oxidation states of thiophene[18b] (0.75 and 1.08 V) and the first oxidation state of thiazole[17c] (0.93 V). The E_{ox}^{onset} of these π-functionalized bithiazole compounds were determined to be 0.94 V for **2Im2TZ**, 0.61 V for **2Py2TZ**, 0.62 V for **2T2TZ**, and 0.35 V for **2TPA2T**, respectively.

Density Function Theory (DFT) Computations. DFT calculations were carried out with the Gaussian09, Revision
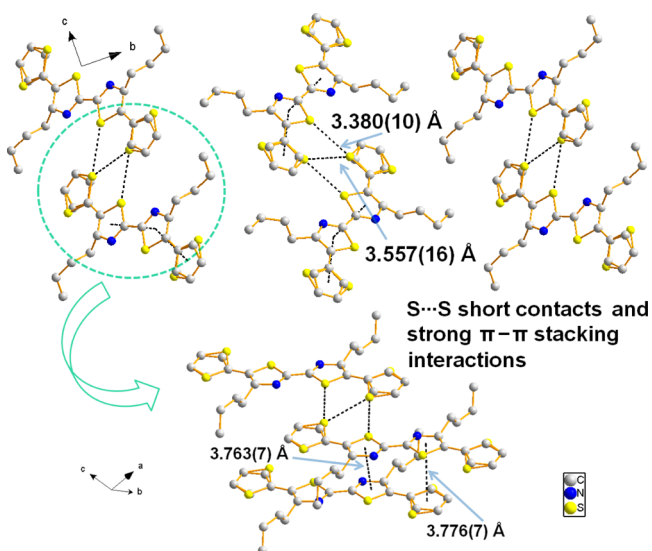
Figure 3. Perspective view of the packing structure in compound 2T2TZ showing the S···S short contacts and strong π−π stacking interactions.
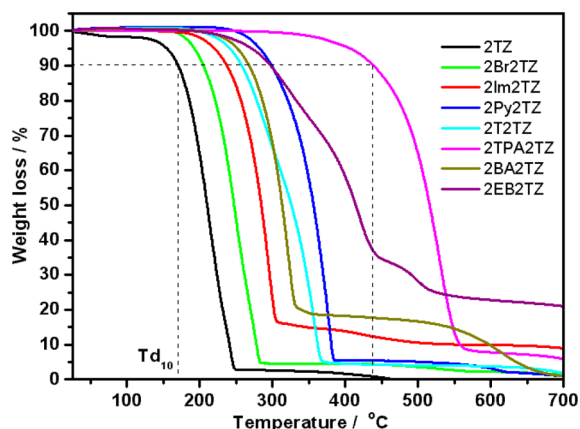

Figure 4. Thermograms of bithiazole-based compounds **2TZ, 2Br2TZ, 2Im2TZ, 2Py2TZ, 2T2TZ, 2TPA2T, 2BA2TZ,** and **2EB2TZ.**
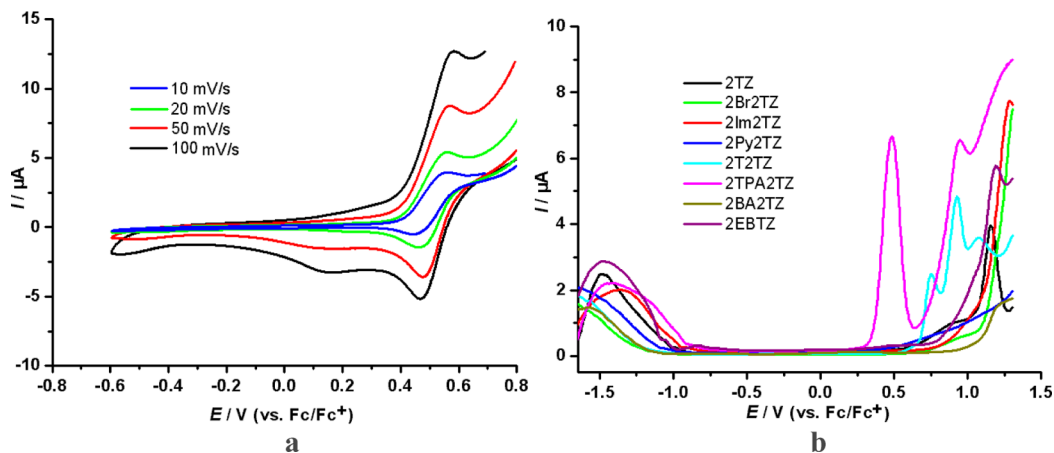
C.01 programs[19] using the B3LYP method and 6-31G* basis set. The fixed atom coordinates of eight bithiazole-based compounds, which are based on the structural parameters determined by the X-ray diffraction method and full optimization, are used for the HOMO and LUMO gap calculations (Table 1).

The resultant HOMO−LUMO gaps for bithiazole-incorporated heterocyclic aromatic compounds **2Im2TZ, 2Py2TZ, 2T2TZ,** and **2TPA2TZ** are 3.84, 3.59, 3.05, and 3.07 eV, respectively, which are analogous to their UV−vis absorption peaks. In addition, the DFT and UV−vis absorption experiments show that compounds **2BA2TZ** and **2EB2TZ** have similar electronic structures. That is to say, the introduction of two ethyl groups on each benzoic acid unit is significant in increasing the solubility in chloroform without impacting the electronic structure.

According to the DPV measurements, further analyses of the frontier orbitals reveal that the introduction of electron-donating groups raises the HOMO energy levels, while the introduction of electron-withdrawing groups lowers the LUMO energy levels, which will greatly decrease the HOMO−LUMO gaps of resultant compounds (see Figure SI12, Supporting Information). It is noted that there is a nearly linear relationship between the experimentally determined energy levels (DPV and UV−vis absorption spectra) and the theoretically calculated ones for the HOMOs and LUMOs of these thiazole/thiophene/imidazole/pyridine heterocyclic aromatic hybrids (Figure 6). This relationship demonstrates that, despite the uncertainty in the calculated absolute values, theoretical calculations can act as a very useful tool to predict and guide the synthesis of future bithiazole oligomer materials.

To make further comparisons from a theoretical and experimental perspective, investigations on the internal reorganization energy (λ) have been done at the B3LYP/6-31G* level for a series of π-conjugated bithiazole-based derivatives and the corresponding bithiophene-based counterparts.[20] Compared with inorganic semiconductors, the charge mobility of organic semiconducting materials is generally determined by a hopping transport process at room temperature.[13b] According to Marcus theory (eq 1),[21] self-exchange rate and the charge mobility are determined by the electronic coupling between adjacent molecules (t) which needs to be
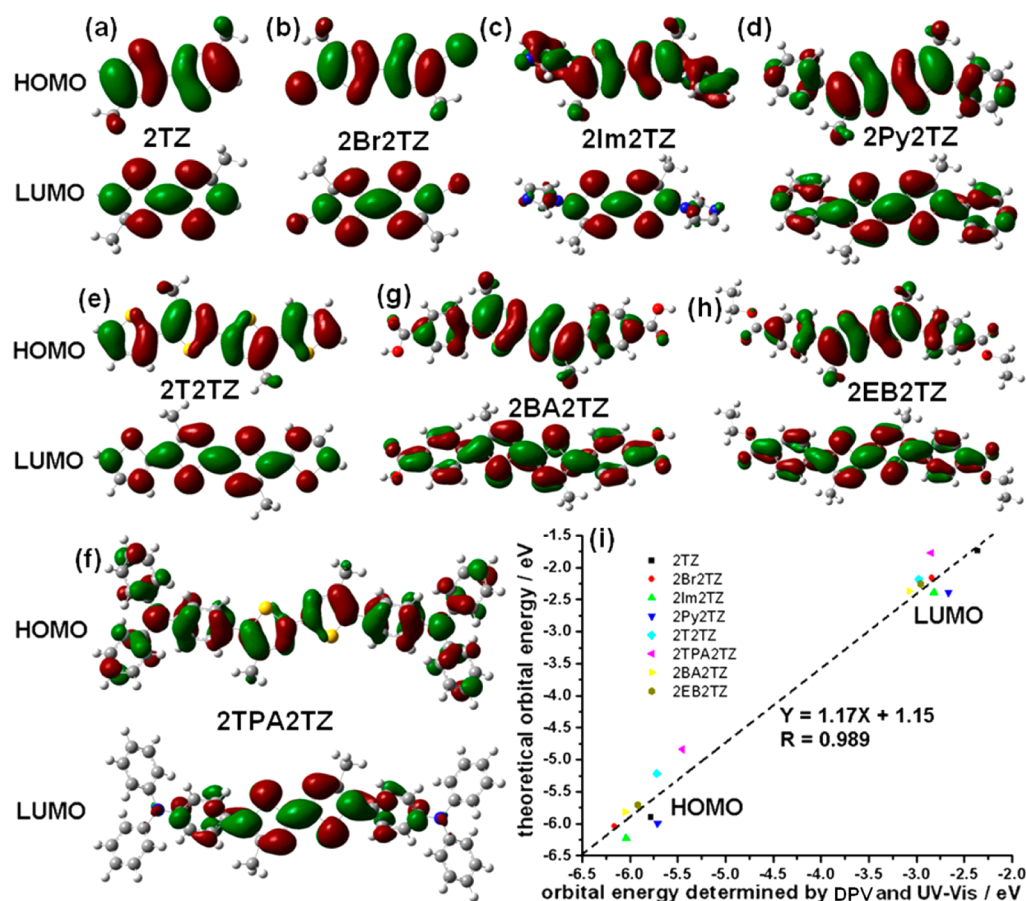

Figure 5. CV (a) and DPV (b) for related heterocyclic aromatic compounds in CH_2Cl_2 (1.0×10^{-3} mol·L^{-1}) containing 0.10 mol·L^{-1} of TBAClO$_4$ under argon. In (a), different scanning rates of 10, 20, 50, and 100 mV/s are used for 2TPA2TZ vs Fc/Fc$^+$.

Figure 6. HOMOs and LUMOs of **2TZ** (a), **2Br2TZ** (b), **2Im2TZ** (c), **2Py2TZ** (d), **2T2TZ** (e), **2TPA2T** (f), **2BA2TZ** (g), and **2EB2TZ** (h) calculated with B3LYP/6-31G*. (i) Energy level correlation between the DPV, UV−vis absorption spectra, and the computational data.

maximized, and the reorganization energy (λ) which needs to be small for efficient charge transport[22]

$$k_{ct} = 4\pi t^2/h(1/4\pi\lambda k_b T)^{1/2}\exp(-\lambda/4k_b T) \qquad (1)$$

where k_b is the Boltzmann constant, h is the Planck constant, and T is the temperature. The reorganization energy (λ) depicts the changes in the geometry of two molecules during the electron transfer reaction.[22] It has two contributions, i.e., an internal one and an external one. The contribution of the environmental factor (intermolecular) to the reorganization energy is expected to be small in organic solids and hence only the intramolecular reorganization energy is calculated.[13b] In this paper, the bithiazole derivatives exhibit slightly larger internal reorganization energy than the bithiophene units. As shown in Table 1, fortunately, these λ values may not seem enormous, which are consistent with those previously reported oligothiophenes[23] (λ = 0.26 eV for α-sexithiophene, λ = 0.29 eV for α-tetrathiophene, and λ = 0.36 eV for α-bithiophene). Comparatively speaking, compounds **2Im2T** and **2Im2TZ** have larger λ values which can be explained commendably by the presence of big dihedral angles between the thiazole/thiophene and the imidazole rings in their crystal structures. Nevertheless, compounds **2Py2T** and **2T2TZ** are predicted to be good candidates for investigations on the design and synthesis of π-conjugated oligomers for OFET materials from a theoretical and experimental perspective.

CONCLUSION

In summary, synthetic, structural, thermal, computational, and spectral comparisons have been carried out for a series of imidazole/pyridine/thiophene/benzene/triphenylamino-containing heterocyclic aromatic fluorescent compounds with the same coplanar bithiazole centers and high stability and solubility. The differences between cross-coupling approaches and experimental conditions on the C−C bond and C−N bond formation, molecular conformation and dihedral angles between neighboring heterocycles, energy gaps and energy levels, and electronic, fluorescent, and electrochemistry spectra have been systematically investigated. X-ray single-crystal structures for this family of multiple *N*-donor containing compounds reveal the same *trans* and coplanar configuration in the bithiazole core with two *n*-butyl chains on each β position but distinguishable dihedral angles between adjacent aromatic heterocycles. Optical and electrochemical results indicate that the TPA-terminated bithiazole compound **2TPA2TZ** has a yellow fluorescent and electrochemical activity. Meanwhile, **2Py2TZ**, **2EB2TZ** and **2TPA2TZ** show excellent performance in the thermal stability. Overall, they may be good candidate molecules toward device fabrication. It is also noted that introducing the two ethyl chains on benzoic acid from **2BA2TZ** to **2EB2TZ** is significant in increasing the solubility, thermal durability and molar extinction coefficient without impacting the electronic structure.

Our theoretical studies are in good agreement with the corresponding photophysical and electrochemical studies. The

internal reorganization energy (λ) for these compounds has been calculated using the B3LYP method and 6-31G* basis set to study their electronic structures and compare the differences between the bithiazole and bithiophene counterparts. This finding highlights the fact that these bithiazole derivatives exhibit slightly larger internal reorganization energy than the corresponding bithiophene units and the variation reorganization behavior is explained commendably by using the molecular planarity and crystal packing model. Further studies are being undertaken on the field-effect, light-emitting, photoresponsive and photovoltaic properties of these linear multiple N-donor containing aromatic heterocycle-based nanowires, nanocomposite films, and nanodevices in our laboratory.

■ EXPERIMENTAL SECTION

Syntheses and Characterizations of the Intermediate Material 1-Bromo-2-hexanone and Heterocyclic Aromatic Compounds 2TZ, 2Br2TZ, 2Im2TZ, 2Py2TZ, 2T2TZ, 2TPA2TZ, 2BA2TZ, and 2EB2TZ. Compound 1-bromo-2-hexanone: This compound was synthesized according to the previously reported literature[12a] by minor modifications. Bromine (15.5 g, 5.0 mL, 97.1 mmol) was added dropwise to a stirred solution of 2-hexanone (9.72 g, 97.1 mmol) in methanol (60 mL) at −10 °C. The mixture was then stirred at 0 °C for 45 min followed by 45 min at room temperature. Water (30 mL) and then concentrated sulfuric acid (50 mL) were added, and the mixture was stirred overnight at room temperature. Water (90 mL) was added, and the mixture was extracted with ether (4 × 50 mL). The combined extracts were washed with aqueous sodium bicarbonate (50 mL) and water (2 × 50 mL). The extracts were dried by anhydrous magnesium sulfate, the solvent was evaporated, and the residue was distilled under reduced pressure to give the compound 1-bromo-2-hexanone (7.28 g, 42%): bp 73−78 °C (18 mgHg); ^{1}H NMR (500 MHz, CDCl$_3$) δ: 3.89 (s, 2H, CH$_2$Br), 2.66 (t, 2H, butyl), 1.59 (m, 2H, butyl), 1.33 (m, 2H, butyl), 0.92 (t, 3H, butyl).

Caution! Although no problem was encountered in all our experiments, the compound 1-bromo-2-hexanone is a kind volatile chemical like tear gas and should be handled carefully.

2TZ. This compound was synthesized according to the previously reported literature[12b] by minor modifications. 1-Bromo-2-hexanone (1.98 g, 11.0 mmol), dithiooxamide (0.60 g, 5.0 mmol), and ethanol (30 mL) were placed in a 100 mL, two-necked, round-bottom flask equipped with a reflux condenser. The solution was heated to reflux for 6 h, and after cooling, it was poured onto the crushed ice. The mixture was extracted with dichloromethane and then dried over anhydrous sodium sulfate. After evaporation of the solvent, the product was obtained as a pale yellow solid in 94%. Yield (1.32 g). The colorless single crystals of **2TZ** suitable for X-ray diffraction measurement were obtained from hexane and dichloromethane (1:1) by slow evaporation in air at room temperature for 2 days. Mp: 64−68 °C. Main FT-IR absorptions (KBr pellets, cm^{-1}): 3421 (b), 3086 (m), 2955 (s), 2855 (s), 1647 (w), 1506 (s), 1456 (m), 1391 (s), 870 (s), 755 (m), 720 (m). ^{1}H NMR (500 MHz, CDCl$_3$) δ: 6.97 (s, 2H, thiazole), 2.83 (t, 4H, butyl), 1.70 (m, 4H, butyl), 1.38 (m, 4H, butyl), 0.96 (t, 6H, butyl). ^{13}C NMR (125 MHz, CDCl$_3$) δ: 160.8, 159.1, 114.5, 31.3, 31.2, 22.3, 13.8. EI-TOF-MS (m/z): calcd for [C$_{14}$H$_{20}$N$_2$S$_2$]$^+$ 280.4, found 280.1. Anal. Calcd for C$_{14}$H$_{20}$N$_2$S$_2$: C, 59.96; H, 7.19; N, 9.99. Found: C, 60.32; H, 7.41; N, 9.76.

2Br2TZ. This compound was synthesized according to the previously reported literature[12c] by minor modifications. Compound **2TZ** (1.40 g, 5.00 mmol) and NBS (1.80 g, 10.1 mmol) were dissolved in a mixture of acetic acid (30 mL) and N,N-dimethylformamide (DMF, 30 mL). After 4 h of stirring in the dark, a solid precipitated in the reaction mixture. The precipitate was filtered, washed with methanol, and then dried to produce compound **2Br2TZ** as white needles after recrystallization from CH$_2$Cl$_2$/hexane (2.02 g, 92%). The colorless single crystals of **2Br2TZ** suitable for X-ray diffraction measurement were obtained from dichloromethane by slow

evaporation in air at room temperature for 3 days. Mp: 70−72 °C. Main FT-IR absorptions (KBr pellets, cm^{-1}): 3398 (b), 2950 (s), 2921 (s), 2858 (s), 1639 (w), 1498 (s), 1444 (s), 1401 (s), 1366 (m), 1093 (m), 1025 (s), 1006 (s), 957 (m), 865 (m), 660 (m). ^{1}H NMR (500 MHz, CDCl$_3$) δ: 2.75 (t, 4H, butyl), 1.68 (m, 4H, butyl), 1.35 (m, 4H, butyl), 0.95 (t, 6H, butyl). ^{13}C NMR (125 MHz, CDCl$_3$) δ: 160.8, 159.0, 114.6, 31.3, 31.2, 22.3, 13.8. EI-TOF-MS (m/z): calcd for [C$_{14}$H$_{18}$Br$_2$N$_2$S$_2$]$^+$ 438.2, found 437.8. Anal. Calcd for C$_{14}$H$_{18}$Br$_2$N$_2$S$_2$: C, 38.37; H, 4.14; N, 6.39. Found: C, 38.52; H, 4.41; N, 6.18.

2Im2TZ: A solution containing compound **2Br2TZ** (0.83 g, 1.90 mmol), imidazole (5.20 g, 76.38 mmol), Cs$_2$CO$_3$ (3.68 g, 11.29 mmol), and anhydrous CuSO$_4$ (16 mg, 0.10 mmol) in DMF (30 mL) was heated to 140 °C for 72 h under argon atmosphere. The reaction mixture was then cooled to room temperature and the solid was removed by filtration and rinsed thoroughly with CHCl$_3$ until no more products could be detected by TLC. The filtrate was concentrated using a rotary evaporator to give brown oil, and the residue was dissolved in CHCl$_3$ (200 mL) and washed thoroughly by brine to remove excess imidazole which could be detected by TLC (iodine fuming). The organic layer was dried by anhydrous MgSO$_4$ and filtered. The organic solvent was removed at reduced pressure. The desired compound **2Im2TZ** was finally separated by silica gel column chromatography using chloroform as an eluent affording yellow solid in a yield of 0.43 g (55%). The yellow single crystals of **2Im2TZ** suitable for X-ray diffraction measurement were obtained from ethyl acetate (EA) by slow evaporation in air at room temperature for 3 days. Mp: 187−189 °C. Main FT-IR absorptions (KBr pellets, cm^{-1}): 3409 (b), 3097 (m), 2907 (m), 1552 (vs), 1475 (m), 1407 (m), 1049 (m), 771 (m), 653 (m). ^{1}H NMR (500 MHz, CDCl3): δ 7.67 (s, 2H, imidazole), 7.25 (s, 2H, imidazole), 7.12 (s, 2H, imidazole), 2.62 (t, 4H, n-butyl), 1.66 (m, 4H, n-butyl), 1.30 (m, 4H, n-butyl), 0.89 (t, 6H, n-butyl). ^{13}C NMR (125 MHz, CDCl$_3$): δ 157.4, 153.2, 138.7, 130.6, 129.6, 121.8, 31.2, 28.1, 22.3, 13.7. EI-TOF-MS (m/z): calcd for [C$_{20}$H$_{24}$N$_6$S$_2$]$^+$ 412.6, found 412.0. Anal. Calcd for C$_{20}$H$_{24}$N$_6$S$_2$: C, 58.22; H, 5.86; N, 20.37. Found: C, 58.01; H, 6.04; N, 20.12.

2Py2TZ. A degassed three-necked flask containing **2Br2TZ** (1.10 g, 2.50 mmol), 4-pyridineboronic acid (0.75 g, 6.00 mmol), [Pd(PPh$_3$)$_4$] (0.12 g, 0.10 mmol), and Cs$_2$CO$_3$ (2.70 g, 8.00 mmol) was dissolved in a degassed mixture of dioxane (50 mL) and H$_2$O (5 mL). The mixture was stirred and refluxed under argon for 48 h. After the mixture was cooled to room temperature, CHCl$_3$ (100 mL) was added, and the organic phase was washed with brine, separated, and dried over anhydrous MgSO$_4$. The organic solvent was evaporated under reduced pressure and the solid residue was purified by silica gel column chromatography using chloroform as an eluent to provide the desired product **2Py2TZ** as light yellow solid in a yield of 0.98 g (90%). The yellow single crystals of **2Py2TZ** suitable for X-ray diffraction determination were grown from a solution of CHCl$_3$ by slow evaporation in air at room temperature for 5 days. Mp: 253−255 °C. Main FT-IR absorptions (KBr pellets, cm^{-1}): 3413 (b), 2927 (m), 1589 (vs), 1543 (w), 1478 (w), 1475 (m), 1407 (m), 819 (m). ^{1}H NMR (500 MHz, CDCl3): δ 8.70 (dd, 4H, J = 6.0, 1.4 Hz, pyridine), 7.40 (dd, 4H, J = 6.0, 1.4 Hz, pyridine), 2.88 (t, 4H, n-butyl), 1.60 (m, 4H, n-butyl), 1.37 (m, 4H, n-butyl), 0.93 (t, 6H, n-butyl). ^{13}C NMR (125 MHz, CDCl$_3$): δ 159.7, 156.1, 150.3, 139.8, 131.4, 123.5, 31.8, 29.7, 22.6, 13.9. EI-TOF-MS (m/z): calcd for [C$_{24}$H$_{26}$N$_4$S$_2$]$^+$ 434.6, found 434.0. Anal. Calcd for C$_{24}$H$_{26}$N$_4$S$_2$: C, 66.32; H, 6.03; N, 12.89. Found: C, 66.11; H, 6.24; N, 12.67.

2T2TZ. To a suspension of magnesium (0.38 g, 16.0 mmol) in anhydrous THF (10 mL), a solution of 2-bromothiophene (2.60 g, 16.0 mmol) in anhydrous THF (10 mL) was added dropwise. The freshly prepared Grignard reagent was then added dropwise to an ice-cooled suspension of compound **2Br2TZ** (1.75 g, 4.00 mmol) and [NiCl$_2$(dppp)] (100 mg) in anhydrous THF (30 mL). The reaction mixture was stirred for 20 h at room temperature. It was then hydrolyzed with a saturated aqueous ammonium chloride solution, and this was followed by the addition of CHCl$_3$ (100 mL). The red organic layer was washed with water (4 × 50 mL) and dried over anhydrous sodium sulfate. The product **2T2TZ** was finally separated by silica gel column chromatography using hexane and dichloromethane (v/v =

1:1) as the eluent. After the removal of solvent and recrystallization from the same solvents, the yellow product was obtained in a yield of 0.95 g (53%). Mp: 207–210 °C. Main FT-IR absorptions (KBr pellets, cm^{-1}): 3418 (b), 2950 (m), 2921 (m), 2858 (w), 2351 (w), 1644 (m), 1493 (w), 1459 (w), 1396 (w), 1050 (w), 689 (m). ^{1}H NMR (500 MHz, CDCl3): δ 7.38 (dd, 2H, J = 5.1, 0.8 Hz, thiophene), 7.20 (dd, 2H, J = 3.6, 0.8 Hz, thiophene), 7.10 (dd, 2H, J = 5.1, 3.6 Hz, thiophene), 2.95 (t, 4H, n-butyl), 1.77 (m, 4H, n-butyl), 1.44 (m, 4H, n-butyl), 0.95 (t, 6H, n-butyl). ^{13}C NMR (125 MHz, CDCl$_3$): δ 157.8, 154.5, 133.0, 127.7, 127.4, 126.5, 114.8, 31.6, 30.0, 22.6, 13.9. EI-TOF-MS (m/z): calcd for $[C_{22}H_{24}N_2S_4]^+$ 444.7, found 443.9. Anal. Calcd for $C_{22}H_{24}N_2S_4$: C, 59.42; H, 5.44; N, 6.30. Found: C, 59.17; H, 5.81; N, 6.08.

2TPA2TZ. A mixture of compound **2Br2TZ** (0.44 g, 1.00 mmol), 4-(diphenylamino)phenylboronic acid (1.16 g, 4.00 mmol), cesium carbonate (1.30 g, 4.00 mmol), $[Pd(PPh_3)_4]$ (0.06 g, 0.05 mmol), toluene (12 mL), and water (3 mL) was degassed for 0.5 h and heated to reflux for 40 h under an argon atmosphere. The mixture was then allowed to cool to room temperature and extracted with chloroform. The resulting organic layer was dried over anhydrous sodium sulfate and filtered. The filtrate was evaporated, and the residue was purified by column chromatography over silica gel using hexane and dichloromethane (v/v = 1:1) as the eluent to give 0.56 g (73%) of compound **2TPA2TZ** as light yellow solid. Mp: 367–370 °C. Main FT-IR absorptions (KBr pellets, cm^{-1}): 3413 (m), 2956 (m), 1589 (s), 1487 (vs), 1330 (m), 1278 (s), 754 (m), 698 (m), 514 (m). ^{1}H NMR (500 MHz, CDCl$_3$) δ: 7.31 (d, 4H, J = 8.2 Hz, triphenylamino), 7.29 (t, 8H, triphenylamino), 7.15 (d, 8H, J = 7.8 Hz, triphenylamino), 7.09 (d, 4H, J = 8.7 Hz, triphenylamino), 7.07(t, 4H, triphenylamino), 2.83 (t, 4H, n-butyl), 1.76 (m, 4H, n-butyl), 1.40 (m, 4H, n-butyl), 0.91 (t, 6H, n-butyl). ^{13}C NMR (125 MHz, CDCl$_3$) δ: 147.3, 130.0, 129.4, 125.0, 123.5, 122.6, 32.0, 29.4, 22.5, 13.9. EI-TOF-MS (m/z): calcd for $[C_{50}H_{46}N_4S_2]^+$ 766.3(100.0), 767.3(56.2), found 766.1(100.0), 767.2(47.8). Anal. Calcd for $C_{50}H_{46}N_4S_2$: C, 78.29; H, 6.04; N, 7.30. Found: C, 77.89; H, 6.51; N, 7.12.

2BA2TZ. A degassed three-necked flask containing **2Br2TZ** (0.88 g, 2.00 mmol), 4-boronobenzoic acid (0.73 g, 4.40 mmol), $[Pd(PPh_3)_4]$ (0.12 g, 0.10 mmol), and Cs$_2$CO$_3$ (1.95 g, 6.00 mmol) was dissolved in a degassed mixture of dioxane (50 mL) and H$_2$O (5 mL). The mixture was stirred and refluxed under argon for 48 h. After being cooled to room temperature, the light yellow solid was obtained in the reaction mixture. The precipitate was filtered, washed with CHCl$_3$ and methanol, and then dried in vacuo to produce compound **2BA2TZ** in a yield of 0.92 g (89%). The yellow single crystals of **2BA2TZ·(DMF)$_2$** suitable for X-ray diffraction measurement were obtained from DMF by slow evaporation in air at room temperature for 3 weeks. Mp: 201–203 °C. Main FT-IR absorptions (KBr pellets, cm^{-1}): 3404 (m), 3138 (s), 3045 (s), 2958 (s), 1693 (m), 1604 (m), 1407 (vs), 1265 (m), 781 (w). ^{1}H NMR (500 MHz, CD$_3$OD) δ: 8.06 (d, 4H, J = 7.8 Hz, phenyl), 7.54 (d, 4H, J = 8.0 Hz, phenyl), 2.85 (t, 4H, n-butyl), 1.75 (m, 4H, n-butyl), 1.36 (m, 4H, n-butyl), 0.91 (t, 6H, n-butyl). ^{13}C NMR (125 MHz, CD$_3$OD) δ: 173.2, 158.6, 154.0, 138.0, 134.2, 133.0, 129.4, 128.5, 31.5, 28.8, 22.0, 12.7. EI-TOF-MS (m/z): calcd for $[C_{28}H_{28}N_2O_4S_2]^+$ 520.7, found 520.1. Anal. Calcd for $C_{28}H_{28}N_2O_4S_2$: C, 64.59; H, 5.42; N, 5.38. Found: C, 64.27; H, 5.68; N, 5.12.

2EB2TZ. A mixture of compound **2BA2TZ** (0.52 g, 1.00 mmol), sodium hydroxide (0.16 g, 4.00 mmol), and ethanol (30 mL) was refluxed for 15 h under argon atmosphere. The mixture was then allowed to cool to room temperature and extracted with chloroform. The resulting organic layer was dried over anhydrous sodium sulfate and filtered. The organic solvent was evaporated under reduced pressure, and the solid residue was purified by silica gel column chromatography using chloroform as an eluent to give 0.39 g (68%) yellow solid of compound **2EB2TZ**. The yellow single crystals of **2EB2TZ** suitable for X-ray diffraction determination were grown from an ethanol solution of sodium hydroxide (10%) by slow evaporation in air at room temperature for 2 weeks. Mp: 171–174 °C. Main FT-IR absorptions (KBr pellets, cm^{-1}): 3401 (b), 2946 (m), 1720 (s), 1606 (m), 1264 (s), 1122 (m), 723 (m), 552 (s). ^{1}H NMR (500 MHz,

CDCl$_3$) δ: 8.12 (d, 4H, J = 8.2 Hz, phenyl), 7.55 (d, 4H, J = 8.1 Hz, phenyl), 4.41 (q, 4H, OCH$_2$), 2.85 (t, 4H, n-butyl), 1.76 (m, 4H, n-butyl), 1.42 (t, 6H, ethyl), 1.36 (m, 4H, n-butyl), 0.90 (t, 6H, n-butyl). ^{13}C NMR (125 MHz, CD$_3$OD) δ: 166.1, 159.2, 155.0, 136.4, 133.1, 130.0, 129.2, 61.2, 31.9, 29.6, 22.5, 14.4, 13.9. EI-TOF-MS (m/z): calcd for $[C_{32}H_{36}N_2O_4S_2]^+$ 576.8, found 576.2. Anal. Calcd for $C_{32}H_{36}N_2O_4S_2$: C, 66.64; H, 6.29; N, 4.86. Found: C, 65.46; H, 6.35; N, 4.62.

X-ray Data Collection and Structural Determination. Single-crystal samples of seven compounds **2TZ**, **2Br2TZ**, **2Im2TZ**, **2Py2TZ**, **2T2TZ**, **2BA2TZ·(DMF)$_2$**, and **2EB2TZ** were covered with glue and mounted on glass fibers and then used for data collection. Crystallographic data were collected on a Bruker SMART 1K CCD diffractometer, using graphite monochromated Mo Kα radiation (λ = 0.71073 Å). The crystal systems were determined by Laue symmetry, and the space groups were assigned on the basis of systematic absences using XPREP.[24] Absorption corrections were performed to all data and the structures were solved by direct methods and refined by full-matrix least-squares method on F_{obs}^2 by using the SHELXTL-PC software package.[25] All non-H atoms were anisotropically refined and all hydrogen atoms were inserted in the calculated positions assigned fixed isotropic thermal parameters and allowed to ride on their respective parent atoms. The summary of the crystal data, experimental details and refinement results for seven compounds is listed in Table 2, whereas bond distances and angles are given in Table SI1 (Supporting Information). In addition, hydrogen-bonding parameters are tabulated in Table SI2 (Supporting Information).

Computational Details. All calculations were carried out with Gaussian 09 programs.[19] The geometries of molecules **2TZ**, **2Br2TZ**, **2Im2TZ**, **2Py2TZ**, **2T2TZ**, **2BA2TZ**, **2EB2TZ** and their respective bithiophene counterparts (see the Supporting Information) were fully optimized and calculated by the B3LYP method and 6-31G* basis set without any symmetry constraints. The single-crystal structures were used as the starting geometries, while other input files were obtained by the substituent-modified approach based on the earlier output files. For computational simplicity, the n-butyl chains are replaced by the methyl groups since this replacement is not expected to alter the results and the trends significantly.[20]

■ ASSOCIATED CONTENT

Ⓢ Supporting Information

Tables of selected bond lengths and angles and intermolecular hydrogen bonds, figures of $\pi-\pi$ stacking interactions, ^{1}H, ^{13}C, ^{1}H–^{1}H, and ^{1}H–^{13}C COSY NMR and EI-TOF-MS spectra, DFT computational details, and electrochemistry diagrams for related compounds. CCDC nos. 914949–914955 for **2TZ**, **2Br2TZ**, **2Im2TZ**, **2Py2TZ**, **2T2TZ**, **2BA2TZ**, and **2EB2TZ**. This material is available free of charge via the Internet at http://pubs.acs.org.

■ AUTHOR INFORMATION

Corresponding Author
*E-mail: whuang@nju.edu.cn.

Notes
The authors declare no competing financial interest.

■ REFERENCES

(1) (a) Roncali, J. *Chem. Rev.* **1997**, *97*, 173–205. (b) Martin, R. E.; Diederich, F. *Angew. Chem., Int. Ed.* **1999**, *38*, 1350–1377. (c) Merlo,

J. A.; Newman, C. R.; Gerlach, C. P.; Kelley, T. W.; Muyres, D. V.; Fritz, S. E.; Toney, M. F.; Frisbie, C. D. *J. Am. Chem. Soc.* **2005**, *127*, 3997−4009. (d) Bazan, G. C. *J. Org. Chem.* **2007**, *72*, 8615−8635. (e) *Molecular Materials*; Bruce, D. W., O'Hare, D., Walton, R. I., Eds.; Wiley-VCH: Weinheim, 2010. (f) Wang, C.-L.; Dong, H.-L.; Hu, W.-P.; Liu, Y.-Q.; Zhu, D.-B. *Chem. Rev.* **2012**, *112*, 2208−2267.

(2) New representative examples: (a) Hamwi, S.; Meyer, J.; Kroeger, M.; Winkler, T.; Witte, M.; Riedl, T.; Kahn, A.; Kowalsky, W. *Adv. Func. Mater.* **2010**, *11*, 1762−1766. (b) Gather, M. C.; Kohnen, A.; Meerholz, K. *Adv. Mater.* **2011**, *23*, 233−248. (c) Hu, T.; He, L.; Duan, L.; Qiu, Y. *J. Mater. Chem.* **2012**, *22*, 4206−4215. (d) Greiner, M. T.; Helander, M. G.; Tang, W.-M.; Wang, Z.-B.; Qiu, J.; Lu, Z.-H. *Nat. Mater.* **2012**, *11*, 76−81.

(3) New representative examples: (a) Osaka, I.; Abe, T.; Shinamura, S.; Miyazaki, E.; Takimiya, K. *J. Am. Chem. Soc.* **2010**, *132*, 5000−5001. (b) Li, Y.-N.; Singh, S. P.; Sonar, P. *Adv. Mater.* **2010**, *22*, 4862−4866. (c) Delgado, M. C. R.; Kim, E. G.; da Silva, D. A.; Bredas, J. L. *J. Am. Chem. Soc.* **2010**, *132*, 3375−3387. (d) Gsanger, M.; Oh, J. H.; Konemann, M.; Hoffken, H. W.; Krause, A. M.; Bao, Z.; Wurthner, F. *Angew. Chem., Int. Ed.* **2010**, *49*, 740−743. (e) Shinamura, S.; Osaka, I.; Miyazaki, E.; Nakao, A.; Yamagishi, M.; Takeya, J.; Takimiya, K. *J. Am. Chem. Soc.* **2011**, *133*, 5024−5035. (f) Wurthner, F.; Stolte, M. *Chem. Commun.* **2011**, *47*, 5109−5115.

(4) New representative examples: (a) Liang, Y.-Y.; Xu, Z.; Xia, J.-B.; Tsai, S.-T.; Wu, Y.; Li, G.; Ray, C.; Yu, L.-P. *Adv. Mater.* **2010**, *22*, 135−138. (b) Delgado, J. L.; Bouit, P. A.; Filippone, S.; Herranz, M. A.; Martin, N. *Chem. Commun.* **2010**, *46*, 4853−4865. (c) Bronstein, H.; Chen, Z.-Y.; Ashraf, R. S.; Zhang, W.-M.; Du, J.-P.; Durrant, J. R.; Tuladhar, P. S.; Song, K.; Watkins, S. E.; Geerts, Y.; Wienk, M. M.; Janssen, R. A. J.; Anthopoulos, T.; Sirringhaus, H.; Heeney, M.; McCulloch, I. *J. Am. Chem. Soc.* **2011**, *133*, 3272−3275. (d) Yella, A.; Lee, H. W.; Tsao, H. N.; Yi, C. Y.; Chandiran, A. K.; Nazeeruddin, M. K.; Diau, E. W. G.; Yeh, C. Y.; Zakeeruddin, S. M.; Gratzel, M. *Science* **2011**, *334*, 629−634. (e) Sun, Y.-M.; Welch, G. C.; Leong, W. L.; Takacs, C. J.; Bazan, G. C.; Heeger, A. J. *Nat. Mater.* **2012**, *11*, 44−48.

(5) (a) *Electronic Materials: The Oligomer Approach*; Mullen, K., Wegner, G., Eds.; Wiley-VCH: Weinheim, 1998; (b) Mishra, A.; Ma, C.-Q.; Bauerle, P. *Chem. Rev.* **2009**, *109*, 1141−1276. (c) Farinola, G. M.; Ragni, R. *Chem. Soc. Rev.* **2011**, *40*, 3467−3482.

(6) (a) *Handbook of Oligo- and Polythiophenes*; Fichou, D., Eds.; Wiley-VCH: Weinheim, 1999. (b) *Handbook of Thiophene-Based Materials: Applications in Organic Electronics and Photonics*; Perepichka, I. F., Perepichka, D. F., Eds.; John Wiley & Sons: New York, 2009.

(7) (a) Price, S. C.; Stuart, A. C.; You, W. *Macromolecules* **2010**, *43*, 797−804. (b) Zhao, Z.-J.; Deng, C.-M.; Chen, S.-M.; Lam, J. W. Y.; Qin, W.; Lu, P.; Wang, Z.-M.; Kwok, H. S.; Ma, Y.-G.; Qiu, H.-Y.; Tang, B.-Z. *Chem. Commun.* **2011**, *47*, 8847−8849. (c) Ie, Y.; Nishida, K.; Kazufumi, M.; Tada, H.; Aso, Y. *J. Org. Chem.* **2011**, *76*, 6604−6610. (d) Bonini, M.; Zalewski, L.; Orgiu, E.; Breiner, T.; Dotz, F.; Kastler, M.; Samori, P. *J. Phys. Chem. C* **2011**, *115*, 9753−9759. (e) Barlow, S.; Risko, C.; Odom, S. A.; Zheng, S. J.; Coropceanu, V.; Beverina, L.; Bredas, J.-L.; Marder, S. R. *J. Am. Chem. Soc.* **2012**, *134*, 10146−10155.

(8) Goel, M.; Jayakannan, M. *Chem.—Eur. J.* **2012**, *18*, 11987−11993.

(9) (a) You, W.; Zhu, H.-Y.; Huang, W.; Hu, B.; Fan, Y.; You, X.-Z. *Dalton Trans.* **2010**, *39*, 7876−7880. (b) Wang, C.-L.; Dong, H.-L.; Li, H.-X.; Zhao, H.-P.; Meng, Q.; Hu, W.-P. *Cryst. Growth Des.* **2010**, *10*, 4155−4160. (c) Burke, K. B.; Shu, Y.; Kemppinen, P.; Singh, B.; Bown, M.; Liaw, I. I.; Williamson, R. M.; Thomsen, L.; Dastoor, P.; Belcher, W.; Forsynth, C.; Winzenberg, K. N.; Collis, G. E. *Cryst. Growth Des.* **2012**, *12*, 725−731.

(10) (a) Huang, W.; Masuda, G.; Maeda, S.; Tanaka, H.; Hino, T.; Ogawa, T. *Inorg. Chem.* **2008**, *47*, 468−480. (b) Wang, L.; You, W.; Huang, W.; Wang, C.; You, X.-Z. *Inorg. Chem.* **2009**, *48*, 4295−4305. (c) Wang, L.; Tao, T.; Fu, S.-J.; Wang, C.; Huang, W.; You, X.-Z. *CrystEngComm* **2011**, *13*, 747−749. (d) Hu, B.; Fu, S.-J.; Xu, F.; Tao, T.; Zhu, H.-Y.; Cao, K.-S.; Huang, W.; You, X.-Z. *J. Org. Chem.* **2011**, *76*, 4444−4456.

(11) (a) Huang, W.; Masuda, G.; Maeda, S.; Tanaka, H.; Ogawa, T. *Chem.—Eur. J.* **2006**, *12*, 607−619. (b) Huang, W.; Tanaka, H.; Ogawa, T. *J. Phys. Chem. C* **2008**, *112*, 11513−11526. (c) Huang, W.; Tanaka, H.; Ogawa, T.; You, X.-Z. *Adv. Mater.* **2010**, *22*, 2753−2758.

(12) (a) Thomas, A. P.; Allott, C. P.; Gibson, K. H.; Major, J. S.; Masek, B. B.; Oldham, A. A.; Ratcliffe, A. H.; Roberts, D. A.; Russell, S. T.; Thomason, D. A. *J. Med. Chem.* **1992**, *35*, 877−885. (b) Yamamoto, T.; Suganuma, H.; Maruyama, T.; Kubota, K. *J. Chem. Soc., Chem. Commun.* **1995**, 1613−1614. (c) Yamamoto, T.; Komarudin, D.; Arai, M.; Lee, B.-L.; Suganuma, H.; Asakawa, N.; Inoue, Y.; Kubota, K.; Sasaki, S.; Fukuda, T.; Matsuda, H. *J. Am. Chem. Soc.* **1998**, *120*, 2047−2058. (d) Wong, W.-Y.; Wang, X.-Z.; He, Z.; Chan, K.-K.; Djurisic, A. B.; Cheung, K.-Y.; Yip, C.-T.; Ng, A. M.-C.; Xi, Y.-Y.; Mak, C. S. K.; Chan, W.-K. *J. Am. Chem. Soc.* **2007**, *129*, 14372−14380. (e) Chen, B.-S.; Chen, Y.-J.; Chou, P.-T. *J. Mater. Chem.* **2011**, *21*, 4090−4094. (f) Kim, H. G.; Jo, S. B.; Shim, C.; Lee, J.; Shin, J.; Cho, E. C.; Ihn, S.-G.; Choi, Y. S.; Cho, K. *J. Mater. Chem.* **2012**, *22*, 17709−17717.

(13) (a) Hutchison, G. R.; Ratner, M. A.; Marks, T. J. *J. Am. Chem. Soc.* **2005**, *127*, 2339−2350. (b) Coropceanu, V.; Cornil, J.; Da Silva Filho, D. A.; Olivier, Y.; Silbey, R.; Bredas, J. L. *Chem. Rev.* **2007**, *107*, 926−952 and references cited therein.

(14) (a) Ibrahim, Y. A.; Al-Awadi, N. A.; Ibrahim, M. R. *Tetrahedron* **2004**, *60*, 9121−9130. (b) Zanitato, P.; Cerini, S. *Org. Biomol. Chem.* **2005**, *3*, 1508−1513. (c) Sarma, M.; Chatterjee, T.; Ghanta, S.; Das, S. K. *J. Org. Chem.* **2012**, *77*, 432−444.

(15) Chen, J. W.; Cao, Y. *Acc. Chem. Res.* **2009**, *42*, 1709−1718.

(16) (a) Johansson, T.; Mammo, W.; Svensson, M.; Andersson, M. R.; Ingans, O. *J. Mater. Chem.* **2003**, *13*, 1316−1323. (b) Bruno, C.; Paolucci, F.; Marcaccio, M.; Benassi, R.; Fontanesi, C.; Mucci, A.; Parenti, F.; Preti, L.; Schenetti, L.; Vanossi, D. *J. Phys. Chem. B* **2010**, *114*, 8585−8592. (c) Ma, C.-Q.; Pisula, W.; Weber, C.; Feng, X.-L.; Mullen, K.; Bauerle, P. *Chem.—Eur. J.* **2011**, *17*, 1507−1518.

(17) (a) Cao, J.; Kampf, J. W.; Curtis, M. D. *Chem. Mater.* **2003**, *15*, 404−411. (b) Zhao, B. T.; Chen, J. Q.; Qu, G. R. *Synth. Met.* **2007**, *157*, 517−522. (c) Lin, Y. Z.; Cheng, P.; Liu, Y.; Shi, Q. Q.; Hu, W. P.; Li, Y. F.; Zhan, X. W. *Org. Electron.* **2012**, *13*, 673−680.

(18) (a) Turbiez, M.; Frere, P.; Roncali, J. *J. Org. Chem.* **2003**, *68*, 5357−5360. (b) Araki, K.; Endo, H.; Masuda, G.; Ogawa, T. *Chem.—Eur. J.* **2004**, *10*, 3331−3340. (c) Collis, G. E.; Campbell, W. M.; Officer, D. L.; Burrell, A. K. *Org. Biomol. Chem.* **2005**, *3*, 2075−2084. (d) Hergue, N.; Frere, P. *Org. Biomol. Chem.* **2007**, *5*, 3442−3449. (e) Kuzuhara, D.; Mack, J.; Yamada, H.; Okujima, T.; Ono, N.; Kobayashi, N. *Chem.—Eur. J* **2009**, *15*, 10060−10069. (f) Balandier, J. Y.; Quist, F.; Amato, C.; Bouzakraoui, S.; Cornil, J.; Sergeyev, S.; Geerts, Y. *Tetrahedron* **2010**, *66*, 9560−9572.

(19) Frisch, M. J. et al.. *Gaussian09, revision C.01*; Gaussian, Inc.: Wallingford, CT, 2010.

(20) Janaki, N. L.; Priyanka, B.; Thomas, A.; Bhanuprakash, K. *J. Phys. Chem. C* **2012**, *116*, 22663−22674.

(21) Marcus, R. A. *J. Chem. Phys.* **1956**, *24*, 966−978.

(22) Mas-Torrent, M.; Rovira, C. *Chem. Rev.* **2011**, *111*, 4833−4856.

(23) Zade, S. S.; Zamoshchik, N.; Bendikov, M. *Acc. Chem. Res.* **2011**, *44*, 14−24.

(24) *SMART and SAINT, Area Detector Control and Integration Software*; Siemens Analytical X-ray Systems Inc., Madison, WI, 2000.

(25) Sheldrick, G. M. *SHELXTL* (Version 6.10). Software Reference Manual; Bruker AXS, Inc.: Madison, WI, 2000.